Kepler Data Release 13 Notes

KSCI-19053-001
Data Analysis Working Group (DAWG)
Tom Barclay (Editor)
Jessie Christiansen (Editor)

Data Release 13 for Quarter Q10

Q.m		First Cadence MJD midTime	Last Cadence MJD midTime	First Cadence UT midTime	Last Cadence UT midTime	Num CINs	Start CIN	End CIN
Q10	LC	55739.343433	55832.765870	27-Jun-2011 08:14:32	28-Sep-2011 18:22:51	4573	39049	43621
Q10.1	SCM1	55739.333557	55769.452008	27-Jun-2011 08:00:19	27-Jul-2011 10:50:53	44220	1159930	1204149
Q10.2	SCM2	55770.290467	55801.737103	28-Jul-2011 06:58:16	28-Aug-2011 17:41:25	46170	1205380	1251549
Q10.3	SCM3	55802.575562	55832.775747	29-Aug-2011 13:48:48	28-Sep-2011 18:37:04	44340	1252780	1297119

Prepared by: ______________________ Date: 2/15/12
Tom Barclay, Kepler Science Office, for the DAWG (next page)

Approved by: ______________________ Date: 2/15/12
Jeffrey Van Cleve, Editor-in-Chief

Approved by: for JMJ by MRH ______________________ Date: 2/15/12
Jon Jenkins, Co-I for Data Analysis & DAWG Lead

Approved by: Michael R. Haas ______________________ Date: 2/15/12
Michael R. Haas, Kepler Science Office Director

Document Control

Ownership
This document is part of the Kepler Project Documentation that is controlled by the Kepler Project Office, NASA/Ames Research Center, Moffett Field, California.

Control Level
This document will be controlled under KPO @ Ames Configuration Management system. Changes to this document **shall** be controlled.

Physical Location
The physical location of this document will be in the KPO @ Ames Data Center.

Distribution Requests
To be place on the distribution list for additional revisions of this document, please address your request to the Kepler Science Office:

Michael R. Haas
Kepler Science Office Director
MS 244-30
NASA Ames Research Center
Moffett Field, CA 94035-1000
Michael.R.Haas@nasa.gov

The Data Characteristics Handbook and accompanying Data Release Notes are the collective effort of the Data Analysis Working Group (DAWG), composed of Science Office (SO), Science Operations Center (SOC) and Guest Observer Office (GO) members as listed below:

Jon Jenkins, Chair
Doug Caldwell, Co-Chair
Barclay, Thomas
Bryson, Stephen T.
Burke, Christopher J.
Christiansen, Jessie L.
Clarke, Bruce D.
Cote, Miles T.
Girouard, Forrest
Haas, Michael R.
Hall, Jennifer
Ibrahim, Khadeejah
Kinemuchi, Karen
Klaus, Todd
Kolodziejczak, Jeffery (MSFC)
Li, Jie
McCauliff, Sean D.
Morris, Rob
Mullally, Fergal
Quintana, Elisa V.
Rowe, Jason
Seader, Shawn
Smith, Jeffrey Claiborne
Still, Martin
Stumpe, Martin C.
Tenenbaum, Peter G.
Thompson, Susan E.
Twicken, Joe
Uddin, Akm Kamal
Van Cleve, Jeffrey

The correct citation for this document is: T. Barclay, J. L. Christiansen, J. M. Jenkins, D. A. Caldwell, S. T. Bryson, C. J. Burke, B. D. Clarke, M. T. Cote, F. Girouard, M. R. Haas, J. R. Hall, K. Ibrahim, K. Kinemuchi, T. C. Klaus, J. J. Kolodziejczak, J. Li, S. D. McCauliff, R. Morris, F. Mullally, E. V. Quintana, J. Rowe, S. Seader, J. C. Smith, M. D. Still, M. C. Stumpe, P. G. Tenenbaum, S. E. Thompson, J. D. Twicken, A. K. Uddin,and J. E. Van Cleve, 2012, Kepler Data Release 13 Notes (KSCI-19053-001).

Contents

A Word of Caution to Users

The Simple Aperture Photometry (SAP) product generated by the PA (Photometric Analysis) pipeline module and the PDC (Pre-search Data Conditioning) processed data are designed for automated photometry on over 160,000 stars. Although significant effort has been expended to make these products robust and reliable, they do not produce the best photometry for every target. To mitigate the impact of non-optimal apertures, Kepler is now providing target pixel files so that users can perform their own photometry. To mitigate known issues with PDC, Kepler has completely reworked this software module and is now producing significantly improved results for most long-cadence targets. To take advantage of these improvements, all quarters of Kepler data will be reprocessed and redelivered to MAST by mid-2012. Meanwhile, cotrending basis vectors (see Section 7.0) have been provided for all past quarters so that users can better remove systematics from the simple-aperture-photometry (SAP) light curves generated by the pipeline or custom light curves self-extracted from the target pixel files.

Investigators are strongly encouraged to study the Data Characteristics Handbook and Data Release Notes for all data sets that they intend to use. We advise against publication of results based on Kepler light curves without careful consideration and due diligence by the end user, and dialog with the Science Office or Guest Observer Office where appropriate.

Users are encouraged to notice and document artifacts, either in the SAP or PDC data, and report them to the Science Office at kepler-scienceoffice@lists.nasa.gov.

Like Waldseemüller's 1507 map, the Maximum A Priori (MAP) method for PDC and other improvements to light-curve correction implemented in Kepler Pipeline 8.0 will show us more of the light-curve world than we knew before, while leaving some hazards to navigation around the edges. Far-ranging light-curve mariners will be given the tools to help navigate in such perilous circumstances by the Guest Observer Office.

1 Introduction

These Data Release Notes provide information specific to the release of Q10 data. These data have been processed with the SOC Pipeline 8.0. These Notes contain the summary figures and tables for this quarter—the companion text can be found in the Kepler Data Characteristics Handbook (KSCI-19040). The sections are numbered in the same order in these Notes and the Handbook to assist the reader, except that Section 5.15 in this document is Section 5.14 in the Data Characteristics Handbook due to the addition of a new Section 5.14.

In addition to this document, many of the features listed here are also flagged in the headers of the FITS data products available from the MAST.

1.1 Dates, Cadence Numbers, and Units

No changes from the Data Characteristics Handbook.

Contents of Data Release 13.

Q.m		First Cadence MJD midTime	Last Cadence MJD midTime	First Cadence UT midTime	Last Cadence UT midTime	Num CINs	Start CIN	End CIN
Q10	LC	55739.343433	55832.765870	27-Jun-2011 08:14:32	28-Sep-2011 18:22:51	4573	39049	43621
Q10.1	SCM1	55739.333557	55769.452008	27-Jun-2011 08:00:19	27-Jul-2011 10:50:53	44220	1159930	1204149
Q10.2	SCM2	55770.290467	55801.737103	28-Jul-2011 06:58:16	28-Aug-2011 17:41:25	46170	1205380	1251549
Q10.3	SCM3	55802.575562	55832.775747	29-Aug-2011 13:48:48	28-Sep-2011 18:37:04	44340	1252780	1297119

2 Release Description

No changes from the Data Characteristics Handbook.

3 Evaluation of Performance

3.1 Overall

The 6.5-h Temporal Median (TM) of the Q10 CDPP time series calculated by the Transiting Planet Search (TPS) pipeline is a measure of noise. Compared to using versions of the pipeline older than the current 8.0, we see a reduction in the median of the value calculated for stars brighter than Kp=12.

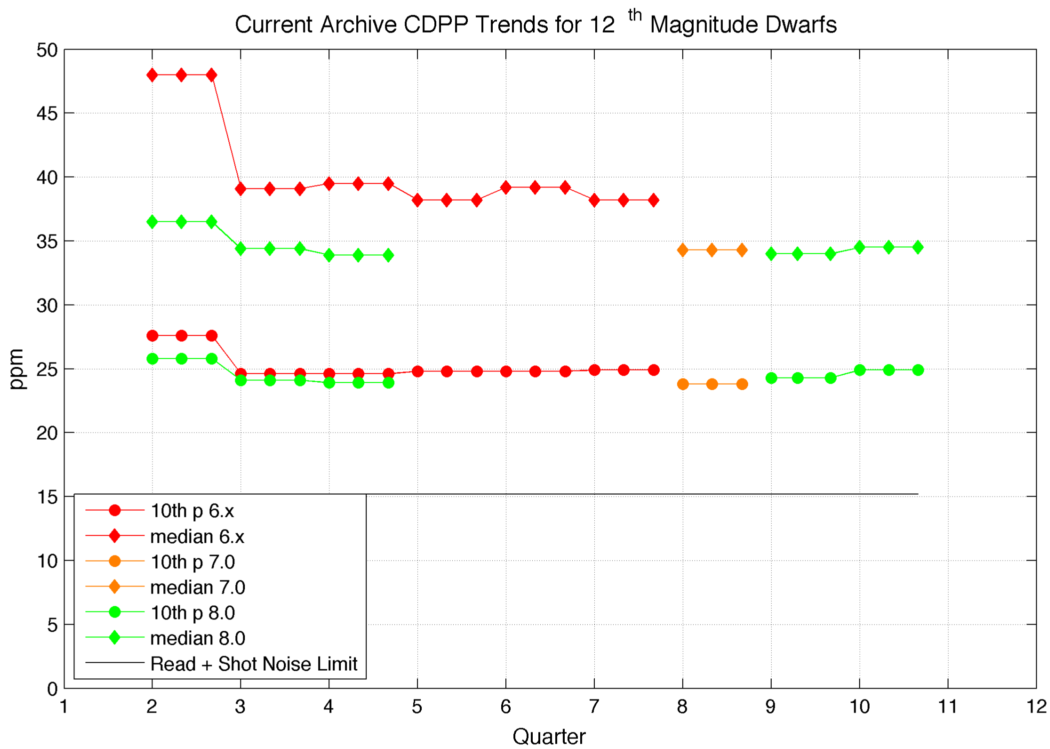

Figure 1: 6.5-h Temporal Median (TM) of the CDPP time series calculated by the TPS pipeline module for dwarf stars between Kp=11.75–12.25. The 6-h TMCDPPs have been divided by sqrt(13/12) = 1.041 to approximate 6.5-h TMCDPPs. A detailed discussion of the median and 10th percentile of CDPP values is given in the Kepler Data Characteristics Handbook. The 6.x, 7.0 and 8.0 labels given in the legend refer to the version of the SOC pipeline used.

Table 1: Aggregate statistics for the TMCDPPs. Column Definitions: (1) Kepler Magnitude at the center of the bin. Bins are ± 0.25 mag, for a bin of width 0.5 mag centered on this value. (2) Number of dwarfs (log g > 4) in the bin. (3) 10th percentile TMCDPP for dwarfs in the bin. (4) Median TMCDPP for dwarfs in the bin. (5) Number of all stars in the bin. (6) 10th percentile TMCDPP of all observed stars in the bin. (7) Median TMCDPP for all stars in the bin. (8) Simplified noise model CDPP.

Kp mag	No. dwarfs	10th prctile	Median	No. stars	10th prctile	Median	Noise model
9.0	56	9.2	22.4	179	11.8	46.6	3.8
10.0	160	12.7	30.1	568	14.0	55.9	6.0
11.0	611	18.2	29.0	1712	19.7	65.3	9.5
12.0	2169	24.9	34.6	4385	26.4	56.6	15.2
13.0	6768	36.6	47.5	10645	38.0	57.9	24.4
14.0	15411	57.9	72.8	18255	58.7	75.9	40.1
15.0	27358	101.5	129.8	27362	101.5	129.8	68.8
16.0	14324	185.8	231.8	14324	185.8	231.8	127.8

4 Historical Events

In this Section, we discuss cadences that may not be useful for high-precision photometry due to planned or unplanned spacecraft events.

4.1 Kepler Mission Timeline to Date

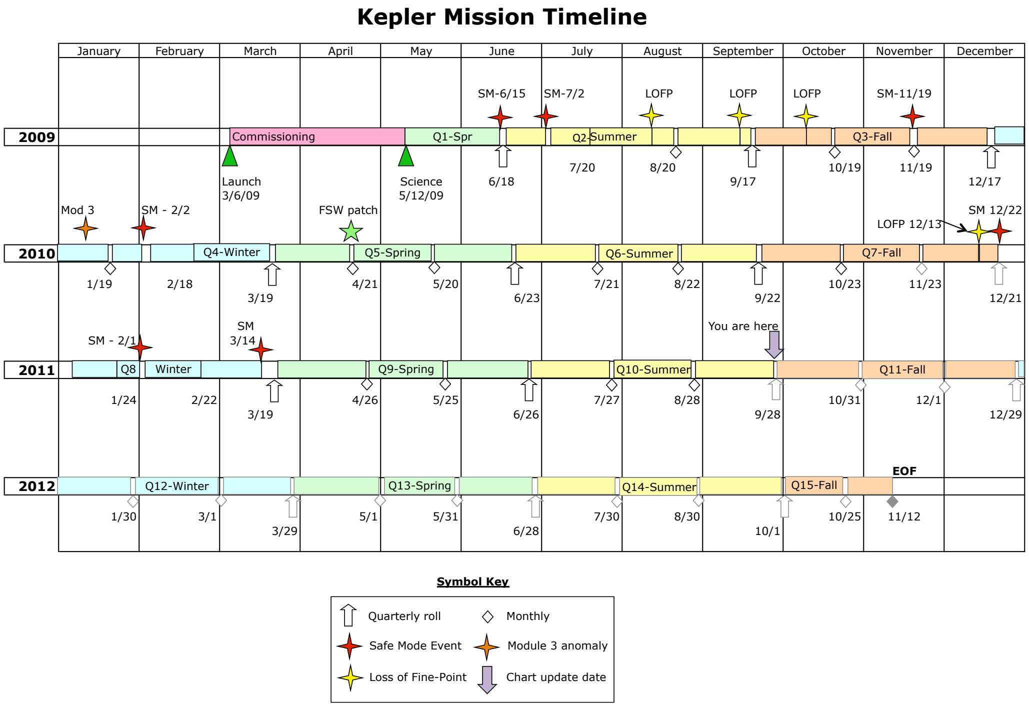

Figure 2: Kepler Mission Timeline as of December 2011.

4.2 Safe Mode

There were no Safe Modes in Q10.

4.3 Loss of Fine Point

The cadences obtained when the spacecraft was not in fine point are listed in Tables 8 and 9, the LC and SC anomaly summary tables, respectively.

4.4 Attitude Tweaks

The pointing history is shown in Figure 3; there were no attitude tweaks during Q10.

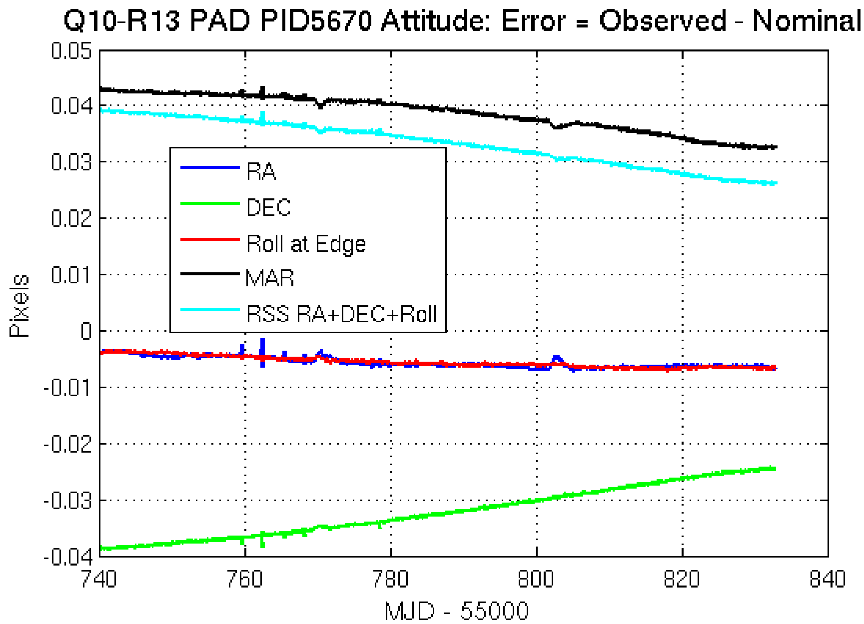

Figure 3: Attitude Error in Q10, calculated by PAD (Photometer Attitude Determination) using Long Cadence data.

4.5 Variable FGS Guide Stars

No changes from the Data Characteristics Handbook.

4.6 Module 3 Failure

No changes from the Data Characteristics Handbook.

5 Ongoing Phenomena

In this Section, we document the systematic errors arising in nominal on-orbit operations, most of which will be removed from the PDC flux time series by the science pipeline.

5.1 Image Motion

The image motion on a per-target basis is now available in the FITS files at MAST via the POS CORR1 (column) and POS CORR2 (row) columns. The column and row motion time series are provided for each mod.out in the Supplement.

5.2 Focus Changes

The change in width of the PRF with time is shown in Figure 4.

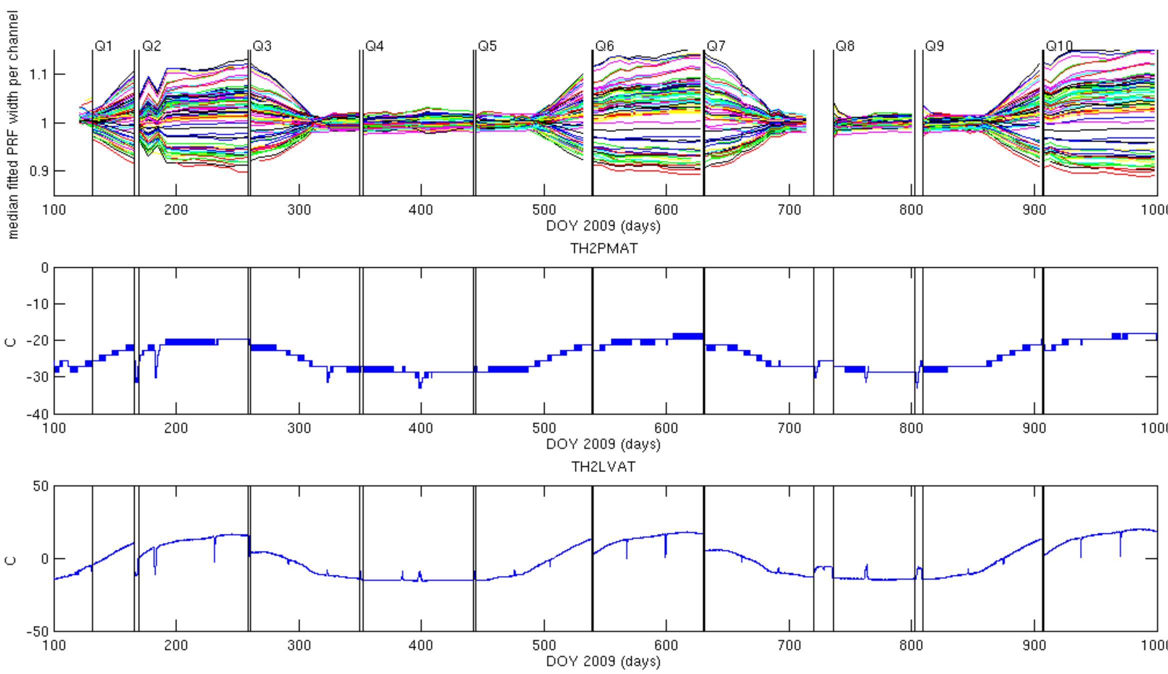

Figure 4: The top plot shows the variation of PRF width with time. The middle and lower plots show the temperature variations of the primary mirror and the launch vehicle assembly. The correlation of the spacecraft temperature and PRF widths demonstrates the seasonal nature of these focus-induced variations.

5.3 Momentum Desaturation

The Long Cadences affected by momentum desaturations in the reaction wheels are listed in Table 2, and the Short Cadences in Table 3. They are also flagged in the FITS files at MAST in the quality flag column (see the Kepler Archive Manual).

Table 2: Momentum desaturations in Q10 and the corresponding Long Cadences. CIN = cadence interval number, RCI = relative cadence index.

LC		
CIN	RCI	Date (MJD)
39152	104	55741.44809
39298	250	55744.43140
39444	396	55747.41471
39590	542	55750.39801
39736	688	55753.38132
39882	834	55756.36463
40028	980	55759.34793
40174	1126	55762.33124
40320	1272	55765.31454
40466	1418	55768.29785
40670	1622	55772.46631
40816	1768	55775.44961
40962	1914	55778.43292
41108	2060	55781.41622
41254	2206	55784.39953
41400	2352	55787.38284
41546	2498	55790.36614
41692	2644	55793.34945
41838	2790	55796.33275
41984	2936	55799.31606
42237	3189	55804.48576
42383	3335	55807.46907
42529	3481	55810.45238
42675	3627	55813.43568
42821	3773	55816.41899
42967	3919	55819.40229
43113	4065	55822.38560
43259	4211	55825.36891
43405	4357	55828.35221
43551	4503	55831.33552

Table 3: Momentum desaturations in Q10 and the corresponding Short Cadences. CIN = cadence interval number, RCI = relative cadence index. The months are separated by horizontal lines.

SC		
CIN	RCI	Date (MJD)
1163030	3101	55741.44503
1163031	3102	55741.44571
1167410	7481	55744.42834
1167411	7482	55744.42902
1171790	11861	55747.41164
1171791	11862	55747.41232
1176170	16241	55750.39495
1176171	16242	55750.39563
1180550	20621	55753.37825
Continued on next page		

Table 3 – continued from previous page

CIN	RCI	Date (MJD)
1180551	20622	55753.37894
1184930	25001	55756.36156
1189310	29381	55759.34487
1193690	33761	55762.32817
1198070	38141	55765.31148
1202450	42521	55768.29479
1208570	3191	55772.46324
1212950	7571	55775.44655
1217330	11951	55778.42985
1221710	16331	55781.41316
1226090	20711	55784.39647
1230470	25091	55787.37977
1234850	29471	55790.36308
1239230	33851	55793.34638
1243610	38231	55796.32969
1247990	42611	55799.31300
1255580	2801	55804.48270
1259960	7181	55807.46600
1264340	11561	55810.44931
1268720	15941	55813.43262
1273100	20321	55816.41592
1277480	24701	55819.39923
1281860	29081	55822.38253
1281861	29082	55822.38322
1286240	33461	55825.36584
1286241	33462	55825.36652
1290620	37841	55828.34915
1290621	37842	55828.34983
1295000	42221	55831.33245
1295001	42222	55831.33313

5.4 Reaction Wheel Zero Crossings

The cadences occurring during reaction wheel zero crossings are listed in Table 4. We note there was an increase in the number of zero crossings during Quarter 10 relative to earlier quarters.

5.5 Downlink Earth Point

The cadences occurring during spacecraft Earth Point are listed in Tables 8 and 9. They are also flagged in the FITS files at MAST in the quality flag column.

5.6 Manually Excluded Cadences

There were no manually excluded cadences in Q10. Any cadences that are manually excluded will be indicated in the quality flag column in the FITS files at MAST.

5.7 Incomplete Apertures Give Flux and Feature Discontinuities at Quarter Boundaries

No changes from the Data Characteristics Handbook.

Table 4: Zero crossing events in Q10, defined as the time from first to last zero crossing in the event, rounded to the nearest cadence. The corresponding Short Cadence numbers can be found in the Data Release 13 Supplement. CIN = cadence interval number, RCI = relative cadence index.

Event no.	MJD start	MJD end	CIN start	CIN end	RCI start	RCI end
1	55741.448	55741.489	39152	39154	104	106
2	55745.984	55747.415	39374	39444	326	396
3	55750.398	55750.521	39590	39596	542	548
4	55756.365	55756.467	39882	39887	834	839
5	55759.430	55759.838	40032	40052	984	1004
6	55762.331	55762.474	40174	40181	1126	1133
7	55765.315	55765.580	40320	40333	1272	1285
8	55768.298	55768.482	40466	40475	1418	1427
9	55775.450	55775.490	40816	40818	1768	1770
10	55778.433	55778.576	40962	40969	1914	1921
11	55828.332	55828.475	43404	43411	4356	4363

5.8 Argabrightening

The cadences affected by Argabrightening events are listed in Tables 5 and 6 for LC and SC respectively. Argabrightenings listed in these tables were detected using the same algorithm as the pipeline, but with a threshold of 10 T_{MAD} instead of the pipeline threshold of 100. Only events exceeding the pipeline threshold are flagged in the FITS files. In short cadence data there was a problem calculating the cadences which experienced Argabrightenings for five functioning channels. Therefore, the maximum number of channels upon which an Argabrightening can be detected in short cadence data is 75.

Table 5: Q10 LC Argabrightening Events with amplitude $T_{\mathrm{MAD}} > 10$, and occurring on a number of channels $T_{\mathrm{MCE}} > 10$. The columns are (1) Cadence interval number (CIN) for Argabrightening cadences, (2) Relative cadence index (RCI) for Argabrightening cadences, (3) Argabrightening cadence mid-times (MJD), (4) Mean Argabrightening statistic over channels included in the Argabrightening event $< S_{\mathrm{Arg}} >_{\mathrm{FPA}}$, (5) Number of channels exceeding threshold for this cadence ($\mathrm{N_{chan}}$), (6) Number of channels exceeding the default pipeline threshold for this cadence ($\mathrm{N_{pipe}}$).

CIN	RCI	Mid-Times (MJD)	$< S_{\mathrm{Arg}} >_{\mathrm{FPA}}$	$\mathrm{N_{chan}}$	$\mathrm{N_{pipe}}$
39080	32	55739.97687	31.1	73	0
39450	402	55747.53731	14.0	72	0
39465	417	55747.84381	9.8	38	0
39756	708	55753.78999	8.6	23	0
40141	1093	55761.65693	8.3	32	0
40490	1442	55768.78826	7.3	11	0
41001	1953	55779.22983	7.6	14	0
41978	2930	55799.19346	2746.5	80	80
41979	2931	55799.21389	81.1	80	15
42005	2957	55799.74517	4.5	18	0
42015	2967	55799.94950	6.2	15	0
42329	3281	55806.36565	24.2	75	0
42330	3282	55806.38609	387.9	80	80
42341	3293	55806.61086	178.0	80	77
42460	3412	55809.04246	7.9	17	0
42485	3437	55809.55330	16.4	70	0
42540	3492	55810.67714	38.0	80	0

Continued on next page

Table 5 – continued from previous page

CIN	RCI	Mid-Times (MJD)	$< S_{\rm Arg} >_{\rm FPA}$	$N_{\rm chan}$	$N_{\rm pipe}$
42619	3571	55812.29140	7.0	12	0
42671	3623	55813.35395	10.0	43	0
42908	3860	55818.19671	8.0	23	0
43407	4359	55828.39308	5.9	11	0
43408	4360	55828.41351	6.7	12	0
43409	4361	55828.43395	6.2	12	0
43412	4364	55828.49525	8.3	28	0
43515	4467	55830.59991	11.4	42	0
43557	4509	55831.45812	608.3	80	80

Table 6: Q10 SC Argabrightening Events with amplitude $T_{\rm MAD} > 10$, and occurring on a number of channels $T_{\rm MCE} > 10$. The columns have the same meanings as Table 5. Note consecutive detections of the largest events. A horizontal line separates the three months of the quarter; the relative cadence index (RCI) is reset at the start of each month.

CIN	RCI	Mid-Times (MJD)	$< S_{\rm Arg} >$	$N_{\rm chan}$	$N_{\rm pipe}$
1160883	954	55739.98266	24.7	62	2
1160885	956	55739.98403	6.7	11	0
1171982	12053	55747.54242	14.6	61	0
1181165	21236	55753.79714	4.2	11	0
1247823	42444	55799.19925	229.6	75	75
1247824	42445	55799.19993	588.1	75	75
1247825	42446	55799.20061	679.3	75	75
1247826	42447	55799.20129	562.3	75	75
1247827	42448	55799.20197	370.2	75	75
1247828	42449	55799.20265	238.5	75	70
1247829	42450	55799.20334	54.3	73	25
1247830	42451	55799.20402	13.8	41	0
1247831	42452	55799.20470	8.2	11	0
1247833	42454	55799.20606	20.9	64	0
1248938	43559	55799.95870	5.0	12	1
1258342	5563	55806.36395	26.8	67	0
1258379	5600	55806.38915	49.7	75	21
1258380	5601	55806.38983	43.0	75	16
1258381	5602	55806.39052	79.9	75	58
1258382	5603	55806.39120	108.0	75	69
1258383	5604	55806.39188	49.4	75	18
1258384	5605	55806.39256	52.0	74	23
1258385	5606	55806.39324	10.2	33	0
1258386	5607	55806.39392	6.6	15	0
1258699	5920	55806.60711	183.3	75	75
1258700	5921	55806.60779	12.0	31	0
1262262	9483	55809.03394	8.1	19	0
1263027	10248	55809.55500	14.5	56	0
1264664	11885	55810.66999	21.3	70	0
1264665	11886	55810.67067	9.5	26	0
1264666	11887	55810.67136	5.2	16	0
1268616	15837	55813.36178	10.1	39	0
1290836	38057	55828.49627	7.5	18	0

Continued on next page

Table 6 – continued from previous page

CIN	RCI	Mid-Times (MJD)	$< S_{\mathrm{Arg}} >$	$\mathrm{N_{chan}}$	$\mathrm{N_{pipe}}$
1293918	41139	55830.59548	8.2	23	0
1295191	42412	55831.46255	85.6	75	62
1295192	42413	55831.46323	142.4	75	74
1295193	42414	55831.46391	186.1	75	75
1295194	42415	55831.46459	158.4	75	73
1295195	42416	55831.46527	35.2	65	15
1295196	42417	55831.46595	5.3	13	0

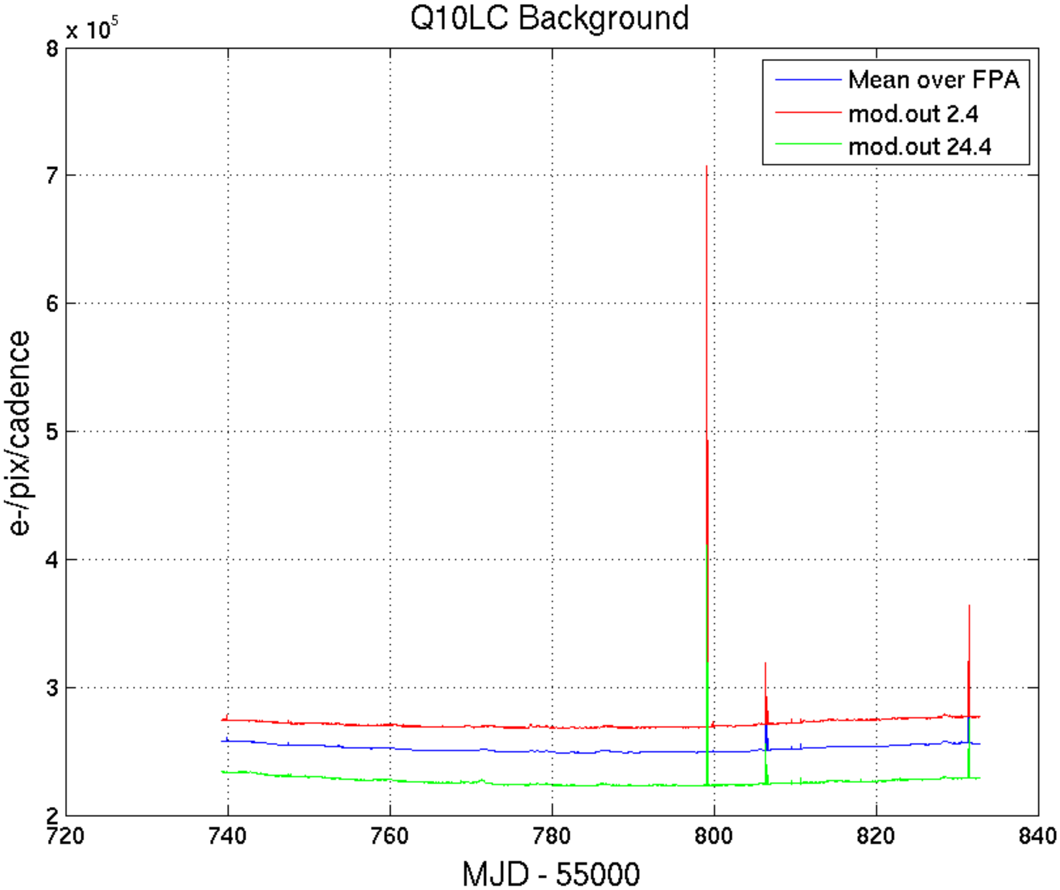

Figure 5: The background flux time series for Q10 showing the average over all the modules, and two individual modules. The focal plane average is shown in blue, modout 2.4 in red and modout 24.4 in green. The narrow spikes are Argabrightening events identified as bad cadences by the Pipeline.

5.9 Background Time Series

The background flux time series for Q10 is shown in Figure 5. We note that due to the presence of faint stars in the pixels used to measure the background flux, there is typically a small over-estimation in the background flux. For very faint targets ($K_p > 18$) this can result in occasional negative flux values in the time series. For brighter targets this has a negligible affect. If this is a concern, users are advised to add the background time series (provided in the FITS files) back to the flux time series, and perform their own background subtraction using appropriate pixels from the target pixel files (see the Kepler Archive Manual for more information).

5.10 Pixel Sensitivity Dropouts

Pixel sensitivity dropouts, such as shown by the red curve in Figure 6, are caused by damage to the CCD crystalline structure by cosmic ray events. The PDC module now identifies and fixes most of these in the PDC light curves as shown as the blue curve in Figure 6. Cadences where these have been identified are flagged in the FITS files (see the Archive Manual for more details).

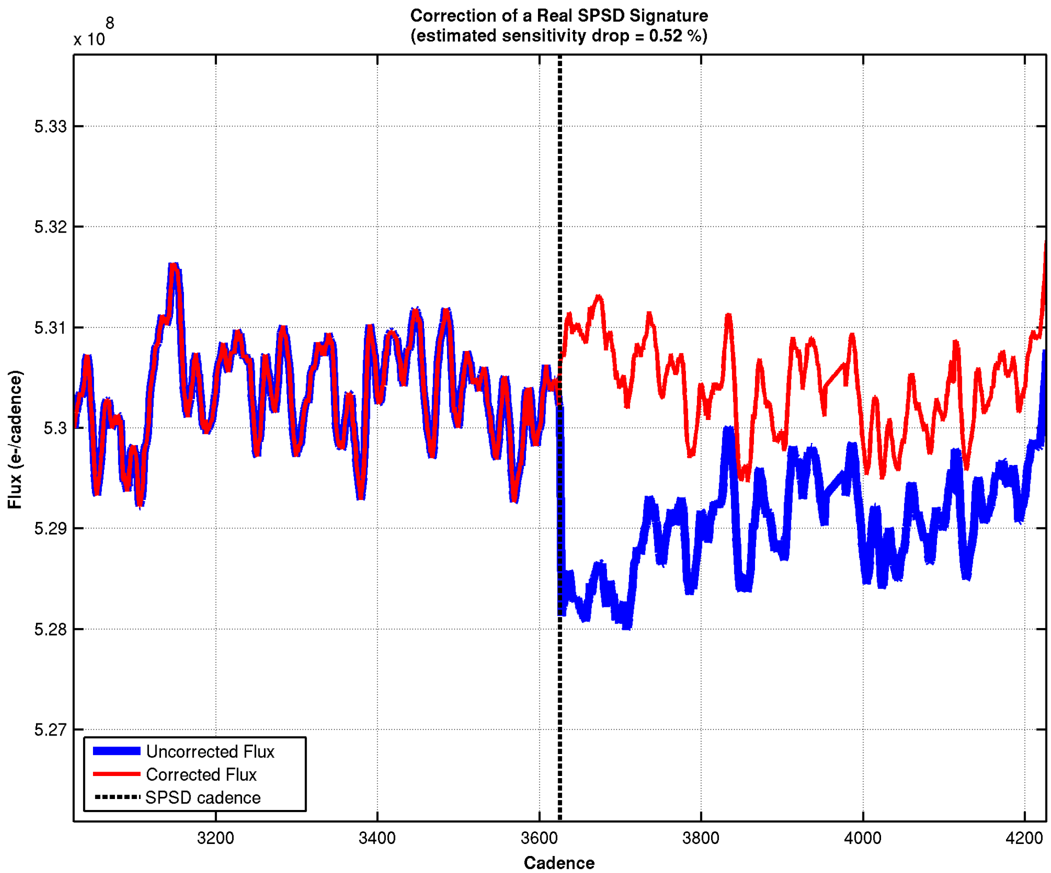

Figure 6: The effect of a sudden pixel sensitivity drop (SPSD). The black dashed line shows the cadence where the SPSD occurs. The blue curve follows the PA data, while the red line shows the PDC correction of the SPSD.

5.11 Short Cadence Requantization Gaps

No changes from the Data Characteristics Handbook.

5.12 Spurious Frequencies in SC Data

A new list of spurious short cadence frequencies was supplied to us by Andrzej Baran of Cracow Pedagogical University. These were not vetted internally by the Kepler Science Office. These frequencies are given in Table 7.

Table 7: Table of additional possible spurious frequencies detected in the SC data. Users are advised to check detections against this list and the list in the Kepler Data Characteristics Handbook, and report additional spurious frequencies. Labels: RW = reaction wheel passive thermal cycle associated with momentum cycle. RWTH = Reaction wheel housing temperature controller thermal cycling (believed not to be a problem from Q3 onward). U = unknown. LC are related to the long cadence read-out frequency. Narrow lines are defined as $\nu/\Delta\nu > 50$, broad lines as $\nu/\Delta\nu < 50$.

frequency	frequency	period	period	period	period			
μHz	d^{-1}	s	min	hr	d	Label	Width	Note
3.9	0.33	112320.00	1872.000	72.000	3.00	RW	?	
86.8	7.50	11520.00	192.000	3.2000	0.133	RWTH	broad	
196.5	16.98	5088.34	84.806	1.4134	0.05889		broad	[6]
242.5	20.95	4124.11	68.735	1.1456	0.04773		very broad	[5]
290.0	25.06	3448.28	57.471	0.9579	0.03991	U1	broad	
340.0	29.38	2941.18	49.020	0.8170	0.03404	U2	broad	
344.9	29.80	2899.33	48.322	0.8054	0.03356		very broad	[4]
360.0	31.10	2777.78	46.296	0.7716	0.03215	U3	narrow	
362.8	31.35	2755.98	45.933	0.7656	0.03190		very broad	[3]
365.8	31.61	2733.31	45.555	0.7593	0.03164		broad	[2]
370.4	32.00	2700.00	45.000	0.7500	0.03125	U4	narrow	
421.0	36.37	2375.30	39.588	0.6598	0.02749	split U5-U8	narrow	
566.4	48.94	1765.56	29.426	0.4904	0.02043	1/LC	narrow	
1132.8	97.87	882.78	14.713	0.2452	0.01022	2/LC	narrow	
1680.1	145.15	595.25	9.921	0.1653	0.00689			[10]
1699.2	146.81	588.52	9.809	0.1635	0.00681	3/LC	narrow	
1803.4	155.81	554.52	9.242	0.1540	0.00642			[1]
1825.2	157.7	547.88	9.131	0.1522	0.00634			[9]
2092.6	180.80	477.88	7.964	0.1327	0.00553			[8]
2265.6	195.74	441.39	7.357	0.1226	0.00511	4/LC	narrow	
2832.0	244.68	353.11	5.885	0.0981	0.00409	5/LC	narrow	
3398.3	293.62	294.26	4.904	0.0817	0.00341	6/LC	narrow	
3964.7	342.55	252.22	4.204	0.0701	0.00292	7/LC	narrow	
4428.4	382.61	225.82	3.763	0.0627	0.00261			
4451.4	384.6	224.65	3.744	0.0624	0.00260			[11]
4531.1	391.49	220.70	3.678	0.0613	0.00255	8/LC	narrow	
4995.8	431.64	200.17	3.336	0.0556	0.00232			[1]
5016.2	433.4	199.35	3.323	0.0554	0.00231			[11]
5097.5	440.43	196.17	3.270	0.0545	0.00227	9/LC	narrow	
5564.4	480.76	179.72	2.995	0.0499	0.00208		broad	[7]
5584.5	482.5	179.07	2.984	0.0497	0.00207			[11]
5663.9	489.36	176.56	2.943	0.0490	0.00204	10/LC	narrow	
6230.3	538.30	160.51	2.675	0.0446	0.00186	11/LC	narrow	
6796.7	587.23	147.13	2.452	0.0409	0.00170	12/LC	narrow	
7024.0	606.87	142.37	2.373	0.0395	0.00165	U5	narrow	[12,16]
7363.1	636.17	135.81	2.264	0.0377	0.00157	13/LC	narrow	
7444.0	643.16	134.34	2.239	0.0373	0.00155	U6	narrow	[13,16]
7865.0	679.54	127.15	2.119	0.0353	0.00147	U7	narrow	[14,16]

Continued on next page

Table 7 – continued from previous page

frequency	frequency	period	period	period	period			
μHz	d^{-1}	s	min	hr	d	Label	Width	Note
7929.5	685.11	126.11	2.102	0.0350	0.00146	14/LC	narrow	
8286.0	715.91	120.69	2.011	0.0335	0.00140	U8	narrow	[15,16]
8495.9	734.04	117.70	1.962	0.0327	0.00136	15/LC	narrow	

[1] Noted in Q7.
[2] 31.52–31.70 d^{-1}, and harmonic at 63.38 c/d.
[3] 31.17–31.53 d^{-1}, noted in Q7.
[4] 29.46–30.14 d^{-1}.
[5] Noted in Q7.
[6] Broad harmonics at 33.95 d^{-1} and 50.92 d^{-1}.
[7] 480.82 d^{-1} in Q6.3, 480.69 d^{-1} in Q7.1, 480.59 d^{-1} in Q7.2, 480.49 d^{-1} in Q7.3.
[8] Noted at 180.45 d^{-1} in Q6.3.
[9] Also noted at 157.97 d^{-1}.
[10] Also noted at 145.36 d^{-1}.
[11] 384.6 d^{-1}, 433.4 d^{-1} and 482.3 d^{-1} have the same separation as the 1/LC artifacts but are shifted from the LC comb by about 6.98 d^{-1}.
[12] Evolved to 609.29 d^{-1} by Q7.1.
[13] Evolved to 645.14 d^{-1} by Q7.3.
[14] Evolved to 680.73 d^{-1} by Q7.3.
[15] Evolved to 716.34 d^{-1} by Q7.3.
[16] These artifacts create a comb with separation 35.7 d^{-1}.

5.13 Propagation of Uncertaintities

No changes from the Data Characteristics Handbook.

5.14 LDE Out of Sync

No cadences were affected by the LDE being out of synchronisation in Q10.

5.15 Anomaly Summary Tables

The full lists of affected cadence interval numbers (CINs) for Tables 8 and 9 below are included in the Data Release 13 Supplement. The Argabrightening Events listed here are those identified by the pipeline and are for completeness only. Those identified at a lower threshold are shown in Section 5.8 and should be considered the most complete list available.

Table 8: Q10 LC Anomaly Summary Table

LC CIN start	LC CIN end	Anomaly Type	Note
39049	39049	EARTH POINT	
40175	40176	COARSE POINT	
40523	40563	EARTH POINT	
41979	41979	COARSE POINT	
42103	42143	EARTH POINT	
43406	43406	ARGABRIGHTENING	

Table 9: Q10 SC Anomaly Summary Table

SC CIN start	SC CIN end	Anomaly Type	Note
1163029	1163040	COARSE POINT	
1167409	1167420	COARSE POINT	
1171789	1171800	COARSE POINT	
1176169	1176180	COARSE POINT	
1180549	1180561	COARSE POINT	
1184929	1184940	COARSE POINT	
1185100	1185130	COARSE POINT	
1189309	1189320	COARSE POINT	
1193689	1193700	COARSE POINT	
1193710	1193769	COARSE POINT	
1194491	1194520	COARSE POINT	
1198069	1198080	COARSE POINT	
1202449	1202460	COARSE POINT	
1206400	1206429	COARSE POINT	
1208569	1208580	COARSE POINT	
1209460	1209489	COARSE POINT	
1211830	1211859	COARSE POINT	
1212760	1212789	COARSE POINT	
1212949	1212960	COARSE POINT	
1217329	1217340	COARSE POINT	
1220380	1220410	COARSE POINT	
1220950	1220979	COARSE POINT	
1221709	1221720	COARSE POINT	
1222330	1222359	COARSE POINT	
1223200	1223229	COARSE POINT	
1225990	1226019	COARSE POINT	
1226089	1226100	COARSE POINT	
1227670	1227699	COARSE POINT	
1228360	1228389	COARSE POINT	
1228870	1228899	COARSE POINT	
1229560	1229589	COARSE POINT	
1230469	1230480	COARSE POINT	
1230700	1230729	COARSE POINT	
1232380	1232409	COARSE POINT	
1233940	1233969	COARSE POINT	
1234540	1234569	COARSE POINT	
1234840	1234869	COARSE POINT	

Continued on next page

Table 9 – continued from previous page

SC CIN start	SC CIN end	Anomaly Type	Note
1237061	1237089	COARSE POINT	
1239190	1239219	COARSE POINT	
1239229	1239240	COARSE POINT	
1240480	1240509	COARSE POINT	
1242340	1242369	COARSE POINT	
1242700	1242729	COARSE POINT	
1243609	1243620	COARSE POINT	
1244050	1244079	COARSE POINT	
1244830	1244859	COARSE POINT	
1247020	1247049	COARSE POINT	
1247830	1247859	COARSE POINT	
1247989	1248000	COARSE POINT	
1248100	1248129	COARSE POINT	
1248160	1248189	COARSE POINT	
1249390	1249419	COARSE POINT	
1249450	1249479	COARSE POINT	
1250260	1250289	COARSE POINT	
1250650	1250679	COARSE POINT	
1251340	1251399	COARSE POINT	
1255579	1255590	COARSE POINT	
1259959	1259970	COARSE POINT	
1262380	1262409	COARSE POINT	
1264339	1264350	COARSE POINT	
1268719	1268730	COARSE POINT	
1270150	1270179	COARSE POINT	
1273099	1273110	COARSE POINT	
1277479	1277490	COARSE POINT	
1281859	1281870	COARSE POINT	
1285570	1285600	COARSE POINT	
1286239	1286250	COARSE POINT	
1287310	1287339	COARSE POINT	
1290619	1290630	COARSE POINT	
1290640	1290669	ARGABRIGHTENING	
1294999	1295010	COARSE POINT	

6 Time and Time Stamps

No changes from the Data Characteristics Handbook.

7 Ensemble Cotrending Basis Vectors

7.1 Introduction

We infer the presence of systematic errors in the Kepler flux time series from the correlations observed between them, since we do not expect the stars themselves to have correlated signals. These correlations can be represented as linear combinations of orthonormal functions, called cotrending basis vectors (CBVs), which in some sense represent most of the correlated features in a reference ensemble of flux time series for a given Quarter and output channel (mod.out). Light curve correction can be performed by finding the 'best' fit of these CBVs to a light curve, and removing the fit. The CBVs of a reference ensemble of highly correlated stars are provided so that users can perform their own systematic error removal without having particular knowledge of proprietary targets, using their own tools or those supplied by the GO office.

In earlier releases, PDC used engineering telemetry and local image motion polynomials derived by the Pipeline itself to remove systematic errors from target flux time series. We have also generated CBVs for these earlier Releases and delivered them to MAST, even though the Pipeline version in use at the time did not use CBVs.

User systematic error correction using the CBVs may be preferable to PDC data, or necessary, since:

1. An ensemble of flux time series is potentially a more complete representation of the trends than engineering telemetry and image motion,
2. Users can decide how many CBVs to use to fit systematic trends,
3. Users can use the CBVs with non-least squares fitting methods such as MAP (Jenkins et al., 2011) or the lasso (Tibshirani 1994; `http://www-stat.stanford.edu/~tibs/ftp/lasso.ps`), and
4. Users of target pixel files who generate their own flux time series will need to do their own systematic error removal, though it is up to the user to understand whether a set of CBVs which well represent systematic errors in uncorrected Pipeline flux time series is also a good representation of their systematic errors given differences in aperture size and their method of extracting a flux time series from the pixels.

7.2 Generation of CBVs

The method for CBV generation in Pipeline 8.0 will be detailed in a future release of the Kepler Data Processing Handbook. Briefly, the method:

1. Removes the median from each uncorrected flux time series,
2. Normalizes each median-removed flux time series by its RMS,
3. Calculates the correlation between RMS-normalized flux time series and selects the 50% most correlated stars as the reference ensemble,
4. Estimates the intrinsic variability of each star in the reference ensemble by removing a 3rd order polynomial fit, and calculating the standard deviation of the detrended light curve normalized by flux uncertainty (roughly, read and shot noise). Stars with a normalized detrended standard deviation 30% greater than the median value on a particular mod.out are rejected from the reference ensemble, and
5. Performs a Singular Value Decomposition (SVD) of the median-removed, median-normalized, variable-cleaned reference ensemble. The CBVs in this case are the SVD principal components, though a more general nomenclature is used to allow non-SVD approaches to be used in the future. Users are provided with the leading 16 components. Users are also provided with the SVD principal values for each mod.out, to inform their decision about how many components to use in their fits.

A good CBV will be representative of many light curves instead of just one or a few. To assess this, we use the robust least-squares fit coefficients for the stars in the reference ensemble, which are generated by the Pipeline as part of the Bayesian Maximum A Posteriori (MAP) method. It can be shown that, for an orthonormal basis, the distribution of fit coefficients is equivalent to the distribution of coefficients that describe the linear combination of light curves which make up each CBV. So a CBV for which a few stars have unusually large fit coefficients is also a CBV which is mostly made up of a linear combination of those few stars' uncorrected light curves, and should not be used. The quantitative metric used to determine the 'quality' of a given CBV is the relative entropy h_i of the probability distribution function p_i of the robust fit coefficients θ_i of the ith CBV, relative to a Gaussian of the same standard deviation:

$$h_i = -\int p_i(\theta_i) \ln p_i(\theta_i) d\theta_i - H_0(\sigma) \tag{1}$$

where

$$H_0(\sigma) = \frac{1 + \ln 2\pi}{2} + \ln \sigma \tag{2}$$

is the entropy of a Gaussian of standard deviation σ.

7.3 Using CBVs

To use the CBVs for least-squares fitting, subtract the median uncorrected flux from the uncorrected flux time series of interest and divide by the median. Since the basis is orthonormal, the linear least-squares fit coefficient of the nth CBV is simply the inner product of the median-removed, median-normalized uncorrected flux time series with the nth CBV. Subtract the fit to get the corrected (median-removed, median-normalized) flux time series.

Convenient CBV tools, including robust fitting and time window exclusion, are provided by the Guest Observer Office as part of PyKE and are available from `http://keplergo.arc.nasa.gov/ContributedSoftwarePyKEP.shtml`. The site provides instructions on how to install the software and specific instructions on how to use the tools to fit the CBVs. Users should note that, unlike the SOC Pipeline, these tools do not include scalar amplitude corrections for the fraction of target flux captured in the optimal aperture, or the fraction of the total flux in that aperture which is from the target star and not from its neighbors or unresolved background objects. These quantities (the flux fraction in aperture and the crowding metric, respectively) are available for the optimal apertures computed by the SOC as keywords in the FITS files at MAST, or for quarters not yet processed by the SOC 8.0 pipline, from the data search page at MAST.

Users will need to use **at least** the first two CBVs, since the generation method mixes a constant offset with the strongest non-constant component instead of strictly enforcing a constant first or second component; using only the first component would be like attempting a linear fit with a constant or slope term, but not both. Figure 7 shows that 8 or fewer components generally capture most of the systematic error for all mod.outs, though 16 are provided if users wish to make their own decisions.

7.4 Quality of CBVs

Generally, CBVs with a relative entropy < -1 should not be used. In Quarter 10 *no* strong CBVs (indices 1–4) are bad, and only 18/320 weak CBVs (indices 5–8) are bad, as shown in Table 10

7.5 Cautions

1. Channels with strong Moiré pattern drift (see the Instrument Handbook, Section 6.7) have less stable weak (>5th order) CBVs, in the sense that random constant perturbations of the reference ensemble give results which differ by significantly more than a constant offset. For good channels, the stability of components to the 10th order has been verified.

2. While most variable stars have been removed from the reference ensemble, it is still possible that some weaker CBVs have been influenced by noisy stars or by variable stars whose signal slips through the detrending filter. Users should exclude bad CBVs from their fits, and in general be cautious about reporting results with the same period and phase as one of the basis vectors used in the fit.

3. No vetting of CBVs 9-16 has been done, as the Pipeline does not generate the robust fit coefficients for these CBVs since they are not used in MAP. These CBVs should be used with extreme caution.

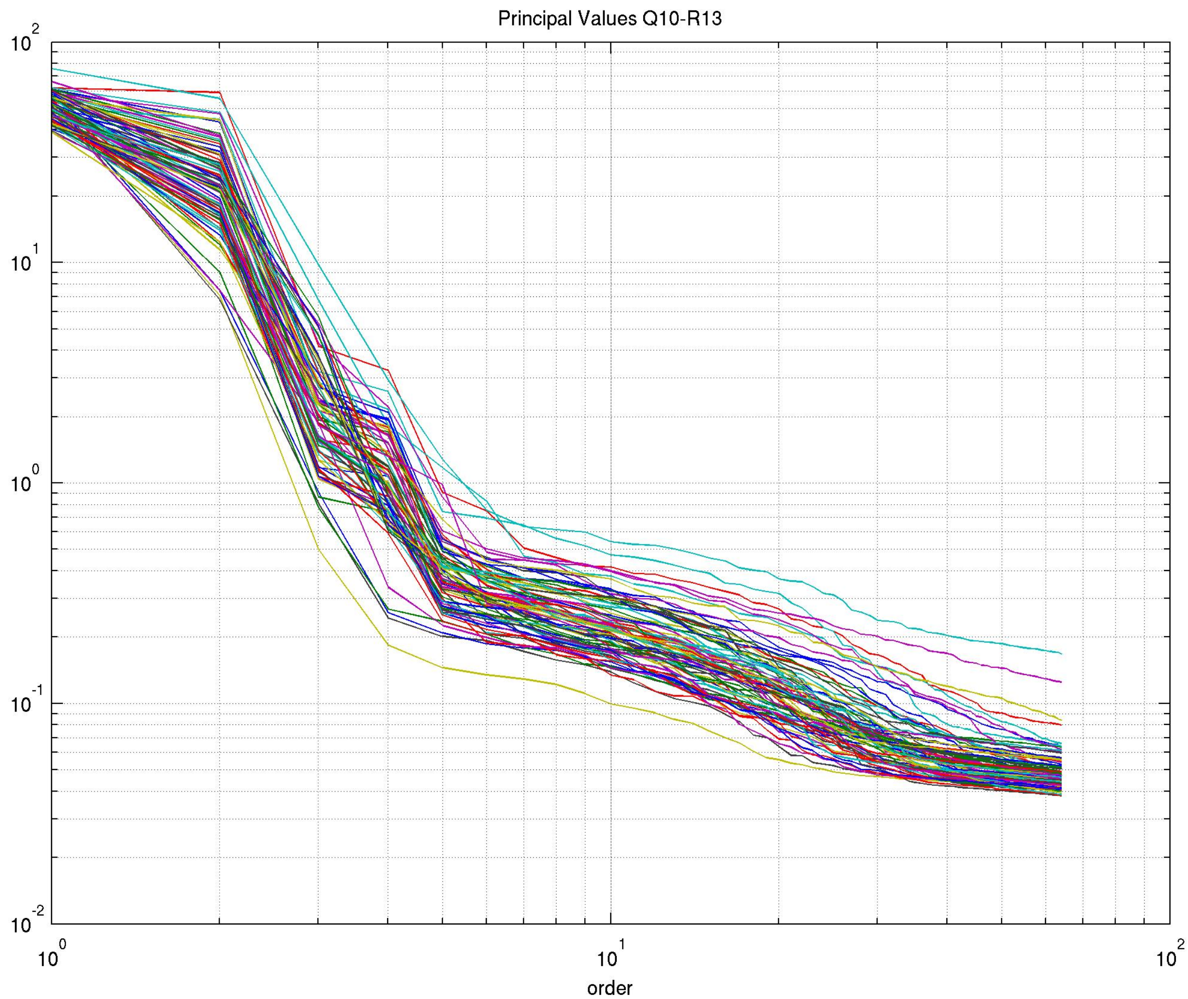

Figure 7: Principal values of SVD-extracted cotrending basis vectors for Quarter 10, Release 13, showing that most of the systematic error can be accounted for by the first 8 or fewer components. Users are provided with the first 16 components for each mod.out, as well as the principal values which are plotted in this Figure.

7.6 Obtaining CBVs

The cotrending basis vectors can be downloaded in FITS files from the MAST website (`http://archive.stsci.edu/kepler`) separate from your data download. There is one file per quarter containing 84 extensions, one for each channel. Each extension contains 16 basis vectors along with the cadence and MJD of the observations. The cadences found in the basis vector file match the number of cadences in the light curve file for that quarter. To ensure that your data was processed through the same version of the pipeline as the stars used to create the basis vectors, the keyword DATA_REL in your data's light curve file should match that found in the basis vector file. A new basis vector file will be provided each time the data are reprocessed.

Table 10: Bad cotrending basis vectors, with relative entropy < -1.

channel	module	output	CBV #	Relative Entropy
4	2	4	7	-1.0398
4	2	4	8	-1.0210
30	10	2	6	-1.1296
31	10	3	6	-1.2347
32	10	4	6	-1.0418
32	10	4	7	-1.0575
37	12	1	7	-1.1342
38	12	2	5	-1.3300
46	14	2	8	-1.4110
47	14	3	8	-1.3039
48	14	4	6	-1.0237
60	17	4	8	-1.4057
75	22	3	5	-1.1494
75	22	3	6	-1.0800
76	22	4	5	-1.0618
76	22	4	6	-1.0038
76	22	4	7	-1.0217
81	24	1	5	-1.3261

8 Contents of Supplement

The Supplement is available as a full package (DataReleaseNotes13SupplementFull.tar), which contains the files described below.

Pipeline Instance Detail Reports

```
q10-lc-ksop-1094-as-run-pipeline-instance-detail-report-111122.txt
q10m1-m2-m3-sc-ksop-1094-as-run-pipeline-instance-detail-report-120127.txt
```

Data Anomaly Types

```
DataAnomalyTypes_Q10LC_LC_PID5670_Summary.txt
DataAnomalyTypes_Q10SCM1_SC_PID5689_Summary.txt
DataAnomalyTypes_Q10SCM2_SC_PID5689_Summary.txt
DataAnomalyTypes_Q10SCM3_SC_PID5689_Summary.txt
```

Mod.out central motion

```
Q10LC_central_column_motion.txt
Q10LC_central_row_motion.txt
```

Thermal Telemetry

```
Q10_LDE_averageBoardTemp.txt
Q10_TH12LVAT_MJD_gap.txt
Q10_TH1RW34T_MJD_gap.txt
```

Background Flux Time Series

```
Q10LC_background.txt
Q10SCM1_background.txt
Q10SCM2_background.txt
Q10SCM3_background.txt
```

Argabrightening Detections

```
Q10LC_LC_ArgAgg_Summary.txt
Q10SCM1_SC_ArgAgg_Summary.txt
Q10SCM2_SC_ArgAgg_Summary.txt
Q10SCM3_SC_ArgAgg_Summary.txt
Q10SCM1_SC_ArgAgg_Summary.txt
```

Out of Fine Point Cadence Lists

```
Q10LC_LC_isNotFinePoint.txt
Q10SCM1_SC_isNotFinePoint.txt
Q10SCM2_SC_isNotFinePoint.txt
Q10SCM3_SC_isNotFinePoint.txt
```

Zero Crossing Events

```
Q10LC_ZeroCrossings.txt
Q10SCM1_ZeroCrossings.txt
```

Q10SCM2_ZeroCrossings.txt
Q10SCM3_ZeroCrossings.txt

Cotrending Basis Vector Entropy and Principal Values

Q10_R13-principal_values_L-0.50_SVDO-8.txt
Q10-R13_bad_entropy_CBVs.txt

8.1 Short Supplement Package

The Supplement also contains a short package suitable for emailing (DataReleaseNotes13SupplementShort.tar). The small package does not contain the following files:

Q10LC_background.txt
Q10SCM1_background.txt
Q10SCM2_background.txt
Q10SCM3_background.txt

Q10LC_central_column_motion.txt
Q10LC_central_row_motion.txt

Q10_TH12LVAT_MJD_gap.txt
Q10_TH1RW34T_MJD_gap.txt

9 References

In addition to those found in the Data Characteristics Handbook:

Jenkins, J. M., Smith, J. C., Tenenbaum, P., Twicken, J. D., and Van Cleve, J., 2011, in Advances in Machine Learning and Data Mining for Astronomy (eds. Way, M., Scargle, J., Ali, K., Srivastava, A.,), Chapman and Hall/CRC Press

Shupe, D. L., et al., 2005, Astronomical Data Analysis Software and Systems XIV, 347, 491

Skrutskie, M. F., et al., 2006, The Astronomical Journal, 131, 1163